

An energy balance climate model with cloud feedbacks

By JOHN O. ROADS and GEOFFREY K. VALLIS, *Scripps Institution of Oceanography, University of California—San Diego, La Jolla, California 92093, U.S.A.*

(Manuscript received January 28; in final form August 1, 1983)

ABSTRACT

A simple two-level global climate model based on the energy balance of the atmosphere and surface is described. The model includes physically based parameterizations for: (1) exchange of heat and moisture across latitude belts and between surface and atmosphere; (2) precipitation and cloud formation; and (3) solar and infrared radiation. Predicted model fields include surface and atmospheric temperature, precipitation, relative humidity and cloudiness. The effects of cloud cover are allowed to feed back into the radiation schemes. In low latitudes, the radiative parameterizations are such that the albedo effects of cloud cover are dominant; in high latitudes, the infrared properties and albedo effects are of equal importance. Several model integrations are described. It is found that cloudiness is generally constant with changing temperature in low latitudes. In high altitudes cloudiness increases with increasing temperature but because of compensating effects on the thermal and solar radiation, the cloud feedback effect on the radiation field is small. The net global feedback by the cloud field is negative but small.

1. Introduction

One characteristic distinguishing the earth from the rest of the planets in our solar system is the presence of a substantial fractional cloud cover, which has conflicting effects on our climate: clouds provide surface warming by decreasing the loss of infrared radiation to space (cloud greenhouse effect), but at the same time give rise to surface cooling by reflecting solar radiation back to space (cloud albedo effect). These compensating feedbacks complicate our understanding of the sensitivity of the earth's climate to various external stimuli, such as increased CO_2 or a variable solar constant, since we still do not know in any detail how the cloud field will change under different climatic conditions.

The radiative effects of clouds, both solar and infrared, have been discussed by London (1957), Rodgers (1967), Ohring and Clapp (1980), Cess and Ramanathan (1978), and many others, although whether the cloud albedo or cloud greenhouse effect dominates or whether these effects mutually compensate is still not yet clear. Schneider (1972) pointed out that an important factor is the behavior of the temperature of the

cloud top compared to the surface and lower tropospheric temperatures. Using average temperatures and cloud top height, Schneider calculated that an increase in cloud cover would cause a global cooling. However, in high latitudes, clouds could provide a surface warming. Namias (1960), and Meleshko and Wetherald (1981), also point out that there may be local and seasonally varying effects. For example, Namias shows that in the continental United States there is an inverse correlation between precipitation (and presumably cloud cover) and surface temperature in the summer and a positive correlation in the winter. However, Cess (1976) has argued that the competing cloud effects may actually compensate each other in all latitude bands and in all seasons. Cess et al. (1982) also discuss the use of satellite data in the problem, and suggest it is yet premature to draw firm conclusions.

While these radiative feedback studies are important for our understanding of the influence of clouds on climate, other studies are equally important to determine the basic reasons for cloud variability. For example, it is by no means certain that even if clouds have a null effect for the present

day climate that they will also have a null effect for other climates. A variety of numerical models showed that a dominant feature of cloud variability was a decrease in middle, tropospheric fractional cloud cover with increasing surface temperature (e.g., MacCracken 1969; Manabe and Wetherald, 1975; Wetherald and Manabe, 1975; Roads, 1978a; Schneider et al., 1979; Wetherald and Manabe, 1980; and Vallis, 1982). In fact, in the GCM study of Wetherald and Manabe (1980), middle latitude and midtropospheric clouds tended to decrease with increasing temperature even though the intensity of the hydrologic cycle (precipitation and evaporation) increased.

Reasons for this decrease in cloud cover were discussed first by Manabe and Wetherald (1975), and later by Roads (1978b), and Wetherald and Manabe (1980). With a more intense hydrologic cycle, the vertical velocity variance tends to increase, resulting in more precipitation in regions of ascent and more drying in regions of descent. In regions of descent, where cloud cover was normally present or under conditions where horizontal advection of dry air is important, the drying effects have more effect on the cloud cover than the moistening effects and, hence, cloudiness decreases with increasing temperature.

However, the vertical velocity variance is not the *only* factor influencing the cloud fields. Roads (1978b) showed that under certain conditions cloud cover can be decreased by increasing the mean downward velocity, by increasing the diabatic heating, by increasing the static stability and by decreasing the scaled evaporation, q_v . Scaled evaporation is the ratio of the surface saturated humidity, q_s^* , to an atmospheric saturated humidity, q_a^* . If temperature alone increases, but lapse rate remains the same, the scaled evaporation decreases, as $\partial/\partial T(q_v) < 0$ for $T_s > T_a$.

This leads to another mechanism affecting the cloud field, discussed by Vallis (1982). Consider the energy balance of the earth's surface, and suppose CO_2 or the solar constant rises forcing the surface temperature to rise. The rapid increase in evaporation (especially at low latitudes) necessitates a fall in sensible heat loss to the atmosphere in order to maintain surface energy balance. This is achieved by an increase in low-level static stability, which, coupled with the consequent decrease in scaled evaporation, causes fractional cloud cover to decrease with increasing temperature.

However, in a GCM experiment, Wetherald and Manabe (1980) found that low-level fractional cloud coverage actually increased with increasing temperature in high latitudes, (similar results were also found by Potter et al., 1981). This occurred over a region in which surface albedo decreased rapidly, due to the retreat of the surface ice-line, causing surface temperatures to rise dramatically—a rise of 19 K was found at latitude 80° in Wetherald and Manabe's model due to a 6% rise in solar constant. Atmospheric temperatures did not rise as rapidly, presumably because of the moderating influences of cross-latitude heat exchange. Vallis (1982) hypothesized that, largely because the ice-albedo feedback was included in Wetherald and Manabe's model, the effective q_v was able to increase and static stability decrease with increasing temperature, thereby causing an increase of cloud amount. Thus, this surface inversion decrease may have been able to completely overwhelm any effect due to changing eddy vertical velocities at low levels.

To test this hypothesis, and to study the influence of cloud feedback on the global climate, we have constructed a simple energy balance model incorporating a parameterization of cloud cover and its radiative feedbacks. The model may be considered an extension of the Budyko–Sellers (Budyko, 1969; Sellers, 1969) type of model to include cloud feedback.

The model does not calculate the vertical velocity explicitly, and the mechanisms described in this paper are based solely on changes in diabatic heating and surface evaporation and precipitation. In building such highly parameterized models, one sacrifices a certain amount of homomorphism with reality, but in return one hopes to isolate the individual operation, and collective effect, of those mechanisms included in the parameterization. Because of the complicated physical processes governing cloud formation and decay, few models, aside from some GCM's, have attempted to incorporate the interactive effects of clouds. The papers by Sellers (1976), Weare and Snell (1974), Paltridge (1975) and Vallis (1982) are exceptions. These models are not physically comprehensive, and one should not regard them as yielding accurate responses to changes in forcing. However, a detailed and careful analysis of a simple model provides useful insight both before and after the analysis of complex GCM's and the natural system.

The model structure is described in Section 2. Section 3 discussed the basic model climate and characteristics. Various perturbation experiments are described in Section 4; conclusions are given in Section 5. We find that, in this model, cloud changes tend to be small, except in high latitudes where surface inversion effect causes an increase in cloud cover with increasing temperature. However, because of the region involved (small area and compensating radiative feedbacks), the effect on the global average temperature is small.

2. Model

Models based on the energy balance of a column of the earth-atmosphere system expressed in terms of the surface temperature have been fairly successful in simulating the zonally averaged surface temperature, but to incorporate cloud feedback requires a more complex model. The model described in this paper is based on the requirements of energy balance at the earth's surface and of the atmosphere, plus the conservation of the water vapor mixing ratio. It is possibly the simplest framework in which the latitudinal variation of surface and atmospheric temperature, and mean cloud cover, may be described, although Paltridge (1975) predicts clouds from apparently fundamental hypotheses, using a simple model.

The choice of atmospheric level in a dry two-level model would naturally be 500 mb, since this temperature most nearly corresponds to the vertically integrated (density weighted) temperature, but because the scale height for water vapor is so small the 500 mb value is not a representative value for water vapor. However, since the temperature lapse rate is more or less constant above the boundary layer, the temperature level is somewhat arbitrary, and we, therefore, use a level of 833 mb to describe an atmospheric value of temperature and mixing ratio. It might seem simpler to use vertically integrated values of temperature and mixing ratio, without specifying a particular level, but in order to derive a relative humidity equation (below), it is necessary to express the mixing ratio and temperature equations at the same levels.

Although predictive equations for temperature and mixing ratio at one atmospheric level (833 mb) and the surface are required, it is convenient to first

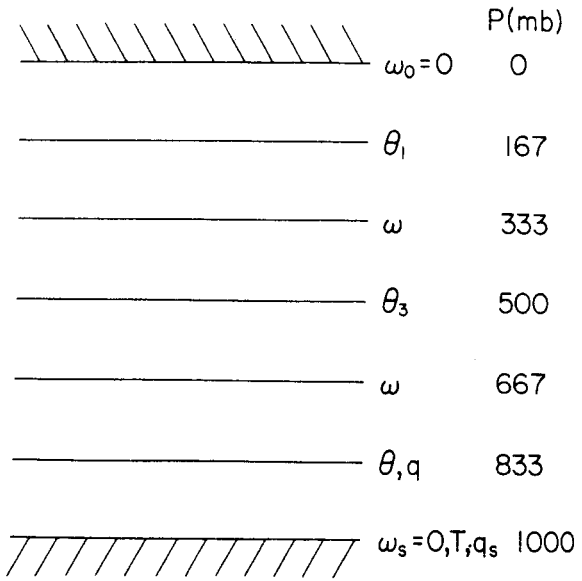


Fig. 1. The vertical structure of the model.

express the variables at three vertical levels, as in Fig. 1. To obtain a single equation for potential temperature at level 5, we assume (1) a constant lapse rate; (2) that the turbulent sensible heat flux from the surface is completely deposited in the lower atmosphere, (3) all water vapor transport and precipitation occurs at the lower level (but through convective overturning the precipitation helps to maintain the lapse rate), and (4) that the radiative flux divergence is a constant, weighted by $(p_i/p_s)^\alpha$, where p_i is the pressure at the i th level, and p_s the surface pressure. Then averaging over all levels and using the continuity equation gives the potential temperature equation at level 5

$$\frac{\partial \theta}{\partial t} = \frac{2\omega \Delta \theta}{p_s} + \frac{g \xi}{C_p p_s} \{F_s - F_0 + S\} + \frac{L \xi}{3 C_p} \dot{p} \quad (1)$$

$$- \frac{(v_1 + v_3 + v)}{3} \cdot \nabla \theta - \nabla \cdot \frac{(v'_1 \theta'_1 + v'_3 \theta'_3 + v' \theta')}{3}$$

the water vapor equation at level 5

$$\frac{\partial q}{\partial t} + \frac{q\omega}{\Delta p} = -\dot{p} + \frac{3gE}{p_s} - v \cdot \nabla q - \nabla \cdot v' q' \quad (2)$$

and the surface temperature equation

$$C_s \frac{\partial T}{\partial t} = -LE - S - F_s \quad (3)$$

where

- θ = potential temperature at level 5
- $\theta_3 = \theta + \Delta\theta$
- $\theta_1 = \theta + 2\Delta\theta$
- $\Delta\theta$ = constant = 20 K
- p_s = surface pressure = $10^5 \text{ kg}^{-1} \text{ s}^{-2}$
- Δp = pressure difference between levels = 333.3 mb
- ω = pressure velocity at level 4 in $\text{kg}^{-1} \text{ s}^{-3}$
- $\xi = (p_s/p_s)^*$
- $\kappa = R/C_p$
- F_s = total surface radiative flux, W m^{-2}
- F_0 = total radiative flux at top of atmosphere, W m^{-2}
- S = surface vertical turbulent eddy heat flux, W m^{-2}
- \dot{p} = precipitation at level 5
- v = mean horizontal velocity at level 5
- q = mixing ratio for water vapor
- E = evaporation or surface vertical turbulent eddy moisture flux
- L = latent heat of condensation = $2.5 \times 10^6 \text{ J kg}^{-1}$
- T = surface temperature
- C_s = surface heat capacity = $1025 \times 10^6 \text{ J m}^{-2} \text{ K}^{-1}$
- $v'\theta'$ = horizontal eddy heat flux
- $v'q'$ = horizontal eddy moisture flux

The model parameterizations will now be described.

2.1. Surface fluxes

We use bulk aerodynamic laws to describe fluxes from the surface into an overlying constant flux layer, obtaining:

$$E = p_s C'_D |v_s| (q_s - q) \tag{4}$$

$$S = p_s C'_D |v_s| (\theta_s - \theta - \Delta\theta_s)$$

where $\Delta\theta_s = -17 \text{ K}$ (see section 3)

C'_D is a drag coefficient

and

ρ_s = surface air density

$|v_s|$ = surface wind speed

We define

$$C_D = \rho_s C'_D |v_s| \frac{g}{p_s}$$

and C_D is given the value 3.10^{-7} s^{-1}

2.2. Solar radiation fluxes

Let the solar properties of the atmosphere be completely described by a single albedo α_a and transmissivity τ_a , and let the surface albedo be α_s . Then the net upward solar fluxes at the top and bottom of the atmosphere (Q_0 and Q_s respectively) are given by a simple application of the adding method (see e.g., Paltridge and Platt, 1976) which accounts for multiple scattering between ground and atmosphere. The results are:

$$Q_0 = -\mu S_0 (1 - \alpha_a - (\alpha_s \tau_a^2 (1 - \alpha_a \alpha_s))) \tag{5}$$

$$Q_s = -\mu S_0 \tau_a (1 - \alpha_s) / (1 - \alpha_a \alpha_s)$$

where μ is an annually averaged cosine zenith angle multiplied by fractional daylight time and S_0 is the solar constant. μ is given by the 5th order polynomial (obtained by a fit to the data of Vernekar (1979)), namely:

$$\mu = \frac{1}{2} \sum_{l=0}^5 a_l x^l$$

where $x = 2y/\pi$ and y is the latitude and $a_l = (0.61632, -0.11209, 0.110536, -2.1097, 2.28883, -0.54153)$.

Ice albedo feedback is incorporated by allowing α_s to increase linearly from 0.1 to 0.7 as temperature falls from 273 K to 263 K. Above 273 K and below 263 K albedo is held fixed at 0.1 and 0.7 respectively.

Atmospheric albedo and transmissivity are functions primarily of cloud cover and type. We allow them to be solely a function of total cloud amount, and derive empirical formulae using the calculations of Rodgers (1967), who gives the net solar radiation at various levels in the atmosphere. Given these, and the surface albedo, it is possible to calculate values for the atmospheric albedo and transmissivity by solving (5) for α_a and τ_a . Using the cloud data of London (1957), linear formula were obtained relating albedo and transmissivity to total cloud cover by a least squares fit. The formulae are

$$\alpha_a = -0.064 + 0.555C \tag{6}$$

$$\tau_a = 0.891 - 0.643C$$

where C is the total fractional cloud cover. Data for all seasons and all latitudes were used. No attempt was made to include the variation of albedo with zenith angle. Fig. 2 illustrates the parameters, and the data used. For cloud amounts less than 0.35 or greater than 0.7, no data exists and the formulae may clearly lead to error. However, such values are never predicted by the model. An idea of the goodness of fit is given by the skill s where

$$s = \left\{ 1 - \frac{\sum_i (y_i - \hat{y}_i)^2}{\sum_i y_i^2} \right\} \times 100\% \quad (7)$$

where y_i is a data point and \hat{y}_i a predicted value using the least squares formulae. For the albedo σ

= 95.4% and for the transmissivity $\sigma = 99.42\%$. With the mean values removed from the y 's in (7) the respective values of σ fall to 45.8% and 63.1%.

2.3. Infrared radiation fluxes

The infrared radiative fluxes at the surface and atmospheric top are described in terms of the surface, one atmospheric temperature field, and the cloud cover. Smagorinsky (1963) proposed one such scheme, which takes the form

$$\begin{aligned} I_0 &= (1 - \Gamma)\sigma T^4 + \nu\uparrow\sigma T_a^4 \\ I_s &= \sigma T^4 - \nu\downarrow\sigma T_a^4 \end{aligned} \quad (8)$$

I_0 and I_s are the net upward fluxes at the surface and 0 mb, and Γ , $\nu\uparrow$ and $\nu\downarrow$ are empirical coefficients. Γ appears to be very constant with latitude; however, $\nu\uparrow$ and $\nu\downarrow$ are very strong

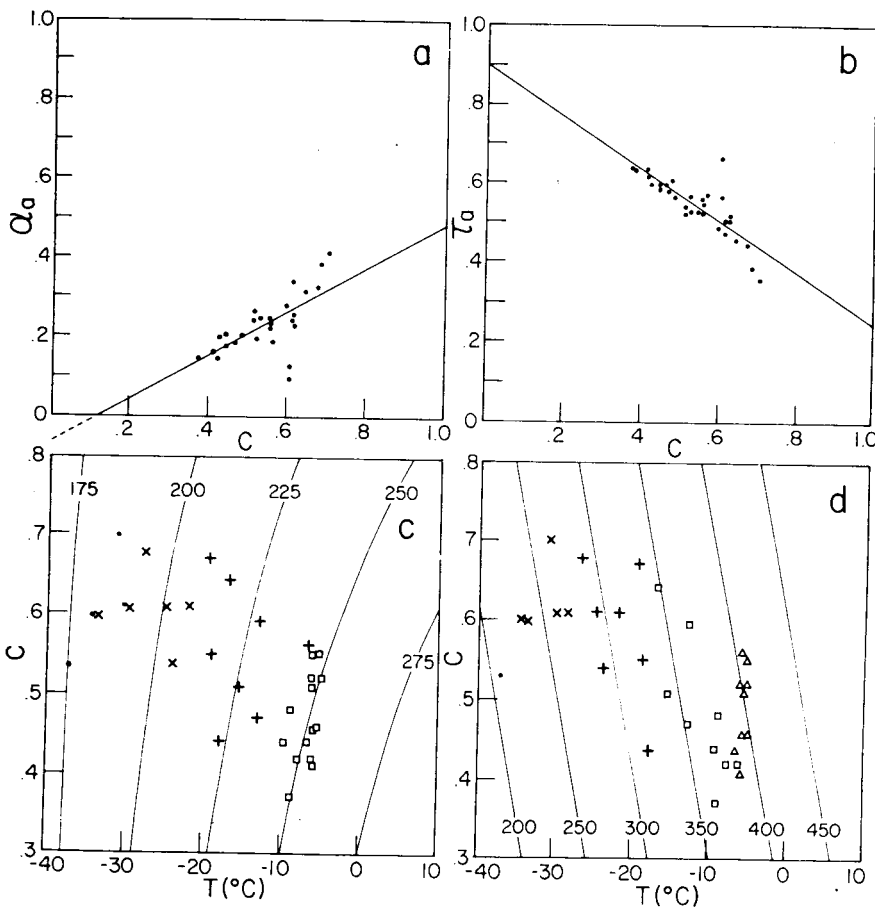


Fig. 2. The least squares fit for the radiative parameters (a) atmospheric albedo, (b) atmospheric transmissivity. (c) upward thermal flux, (d) downward thermal flux. In (c) and (d) the values of the flux for the least square fit are given on the iso-flux lines. The symbols (\cdot , \times , $+$, $[\]$, Δ) denote actual values of (175, 200, 225, 250, ... ± 12.5) in (c) and (200, 250, 300, 350, 400 ... ± 25) in (d).

functions of latitude. We therefore use a parameterization of the form

$$I_0 = (1 - \Gamma)\sigma T^4 + (A\uparrow + B\uparrow T_a)(1 - C) + (A'\uparrow + B'\uparrow T_a)C \quad (9)$$

$$I_s = \sigma T^4 - (A\downarrow + B\downarrow T_a)(1 - C) - (A'\downarrow + B'\downarrow T_a)C$$

We again use the data of Rodgers (1967) for all latitudes and seasons to obtain least squares fits to give the constants A and B . The value of Γ is 0.96, from Smagorinsky (1963), and the A 's and the B 's are (for T_a in °C)

$$(A\uparrow, B\uparrow, A'\uparrow, B'\uparrow) = (293.7, 3.084, 227.6, 1.377)$$

$$(A\downarrow, B\downarrow, A'\downarrow, B'\downarrow) = (374.8, 6.347, 494.4, 6.285)$$

T_a is the 500 mb atmospheric temperature, $\{(\theta + \Delta\theta)/(p_s/p_3)^{\kappa}\}$, and C the total cloud cover. The parameters and data are also illustrated in Fig. 2. The formulae show that outgoing radiation to space varies more slowly with temperature as cloud cover increases, although the downward radiation changes little. Note also that the slopes of the lines seem to be physically reasonable. The value of s for the upward atmospheric flux is 99.97% and 99.95% for the downward. On removing the means these values drop to 97.3% and 98.5% respectively. As only one cloud layer is predicted we are unable to explicitly model any changes in cloud top height, except insofar as this may implicitly be modelled by (9).

2.4. Horizontal eddy fluxes

We assume that the horizontal transport of heat and moisture can be described by simple diffusion laws—a common assumption in simple climate models (e.g., North, 1975), although its theoretical foundations are insecure (see Green, 1970).

$$-\frac{(v_1 + v_3 + v)}{3} \cdot \nabla\theta - \nabla \cdot \frac{(v'_1\theta'_1 + v'_3\theta'_3 + v'\theta')}{3} = K\nabla^2\theta \quad (10)$$

and
$$-v \cdot \nabla q - \nabla \cdot v'q' = K\nabla^2 q$$

We use a constant value for K , namely

$$K = 3 \times 10^6 \text{ m}^2 \text{ s}^{-1}$$

Note that the heat transport due to the mean meridional circulation is essentially treated explicitly, through the first term on the right-hand side

of (1). See also the model heat balance in Fig. 6. We make the further approximation that the dominant horizontal variations in the mixing ratio are due to changes in the temperature and, thus, in the saturation mixing ratio rather than in the relative humidity, and hence:

$$K\nabla^2 q \sim KH \frac{\partial q}{\partial \theta} \nabla^2 \theta \quad (12)$$

where $H = q/q^*$ and q^* = saturation mixing ratio at θ and P_s . As shall be shown below, this assumption simplifies the calculations for the moisture variables.

2.5. Cloud cover precipitation and relative humidity

It is natural to scale the water vapor equation by the saturated mixing ratio, and to derive an equation for relative humidity. This is also convenient for the precipitation and cloud cover parameters. The derivation is similar to Roads (1978b) and leads to the three-dimensional relative humidity equation:

$$\frac{\partial H}{\partial t} + q_\beta \omega H = -\dot{P}q_\delta + 3C_D(q_\gamma - H) - H \frac{q_\alpha g}{pC_p} \{F_s - F_0 + S\} \quad (13)$$

where:

$$q_\alpha = \frac{\partial}{\partial \theta} \ln q$$

$$q_\beta = \frac{1}{\Delta P} \left\{ 1 + 2 \frac{q_\alpha \Delta \theta}{3} \right\}$$

$$q_\gamma = q_s^*/q^*$$

$$q_\delta = \left\{ \frac{1}{q^*} + \frac{Lq_\alpha}{3C_p} \right\}$$

and the superscript * indicates the saturation value. The horizontal eddy flux of relative humidity is identically zero following from the assumption of (12).

Using (13), it is possible to derive equations not only for the zonally averaged relative humidity but also for the zonally averaged fractional cloud cover and precipitation. The parameterizations (described in detail in Roads, 1978b and based on the inter-

actions of a zonally varying relative humidity wave with a vertical velocity wave) lead to the formulae:

$$C = 1 - \cos^{-1}(B/W)/\pi \tag{14}$$

$$\dot{p} = \frac{Wq_\beta}{q_\delta} \left\{ \frac{1}{\pi} \sin \pi C - C \cos \pi C \right\} \tag{15}$$

$$H = C + \int_{-\pi(1-C)}^{\pi(1-C)} \frac{d\phi\eta}{(\eta + \cos \pi C + \cos \phi)} \tag{16}$$

where $\eta = 3C_D q_\gamma / Wq_\beta$ and where W is the amplitude of a vertical velocity wave, varying zonally as $W \cos \phi$, with ϕ the longitude. B is a collection of terms involving the mean atmospheric heating, scaled evaporation and mean vertical motion and is:

$$B = \frac{1}{q_\beta} \left\{ 3C_D(q_\gamma - 1) - \bar{\omega}q_\beta - \frac{q_a g \zeta}{C_p p} \times \{F_s - F_0 - S\} \right\}$$

where $\bar{\omega}$ is the zonally averaged vertical pressure velocity (see Fig. 3). Eqs. (14), (15) and (16) are

used in place of (13) and together with (1) and (3) form the model. It is to be emphasized that (14), (15) and (16) are parameterizations based on a simple model which prescribes a fixed longitudinal structure for the atmosphere at all latitudes. Such a parameterization is required because the zonally-averaged mixing ratio cannot directly be used to predict cloud cover and precipitation in the same way as is used, for example, in a high resolution GCM. Also for the purposes of the radiation schemes we have assumed the parameterization gives total cloud cover, and not simply low cloud. The scheme is an over-simplification, but it does enable explicit analyses to reveal those important factors determining cloud variability within the parameterization schemes.

In the derivation, the local time derivative and horizontal advection of relative humidity are neglected and because of this the integral values of precipitation and evaporation do not always exactly balance. At each timestep a correction was applied equally to precipitation and evaporation weighted with the cosine of latitude. This correction was always small.

2.6. Differencing

The zonally-averaged model was solved on a horizontal grid extending from the equator to the pole in 5° increments (from 2.5° to 87.5°). An explicit forward time step was used to iterate the model toward a stationary state. For the control run and for the experiments to be described later, approximately one year of simulated time was required in order to achieve a steady state. This time was set predominantly by the surface heat capacity—if smaller surface heat capacities were used then the time step had to be proportionately smaller. The value of the heat capacity is irrelevant to the final steady state. For these experiments a time step of ¼ day was sufficient for stability. Because a time-marching scheme was used, all solutions found are stable equilibria.

3. Equilibrium results

In a model of this nature certain parameters must be tuned since their exact values are not well known. In this model these parameters were the drag coefficient, the eddy and mean (W and $\bar{\omega}$) vertical velocity magnitudes, the potential temperature correction value and the large-scale eddy

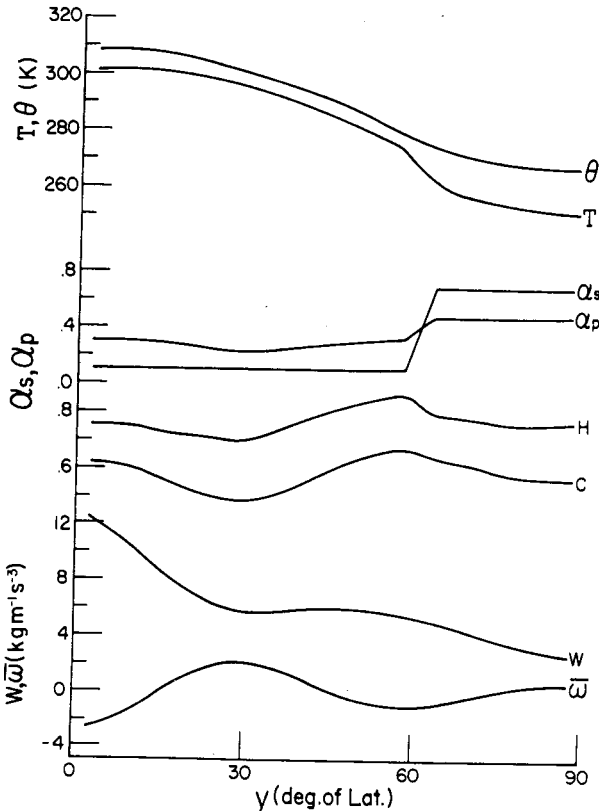


Fig. 3. Model parameters for the control run as a function of latitude.

diffusivity constant. Values for the tuned constants were given in the previous section and Fig. 3 illustrates the preset eddy vertical velocity amplitude and zonal mean vertical velocity profile. This profile helps to determine the gross variation of the latitudinal cloud distribution. Using these values, the model was integrated from isothermal initial conditions to a steady state (a variety of initial conditions was in fact used in a search for multiple solutions. Except for the effect of ice-hysteresis, discussed below, all solutions found were independent of initial conditions).

Fig. 3 shows the equilibrium value's potential temperature at 833.3 mb, θ , surface temperature T , surface albedo α_s , planetary albedo α_p , relative humidity H , and fractional cloud cover. Mean values are given in Table 1. These values resemble the observed values. Note in particular a strong polar inversion, relative maxima of cloud cover and relative humidity in the tropic and mid-latitudes, and the maximum of meridional temperature gradient in mid-latitudes.

It is of interest to determine the contribution by various mechanisms to the cloud cover. Fig. 4 shows B_1 , B_2 and B_3 which refer to the contribution to B by the scaled evaporation, the mean

circulation and the diabatic heating. The dominant latitudinal variation is due to the change in mean circulation, i.e., the effects of the Hadley and Ferrel cells. In high latitudes the effect of diabatic heating is the largest single contribution. However, as will be shown, the changes in cloud cover are caused mainly by changes in the scaled evaporation.

The variations in the surface heat and radiative fluxes are displayed in Fig. 5. In low latitudes the surface balance lies essentially between evaporation and solar flux, whereas in high latitudes the infrared flux balances the solar input. A global balance is achieved in the steady state between incoming solar and outgoing infrared radiation (see also Table 1 and Table 2).

The atmospheric heat balance is illustrated in Fig. 6. In low latitudes the dominant balance lies between precipitation and infrared radiation; in polar regions the horizontal eddy heat flux is balanced by outgoing infrared radiation. However, note that all terms are important.

3.1. *Some radiative calculations*

In this section we explore the radiative effects of the cloud cover. A convenient parameter to

Table 1. Globally averaged values for various terms and for various experiments with the model. $I_0, Q_0, Q_s, E, S, I_s, \delta$ are given in units of $W m^{-2}$ and the terms contributing to the atmospheric heat balance, $P, Solar, Thermal, S$ are given in units of $K/(10^5 s)$. $\Delta S = 2, -2$ refer to the sensitivity experiment with a +2, -2% change in solar constant. Dashes indicate that these particular parameters were not calculated for a particular experiment. The cloud values predicted for $c = 0.5$ and 0.6 are used only in the hydrology cycle.

	Control	C = .5	C = .6	$\Delta S = 2$	$\Delta S = -2$
θ	295.1	300.0	291.9	298.2	291.7
T	288.1	292.1	285.3	290.8	285.0
α_s	.1808	.1562	.2085	.1624	.2085
α_a	.3083	.3017	.3155	.3034	.3155
H	.7599	.7573	.7576	.7606	.7577
C	.5748	.5768	.5711	.5776	.5710
I_0	239.8	—	—	245.7	233.3
Q_0	-239.8	—	—	-245.7	-233.3
Q_s	-157.5	-172.5	-148.3	-162.4	-151.7
E	77.47	90.6	68.7	86.09	68.19
S	30.53	27.5	31.5	29.10	31.62
I_s	49.52	54.4	48.06	47.2	51.90
P	.8041	.9405	.7132	.8936	.7079
Solar	.8543	.8273	.8733	.8653	.8466
Thermal	-1.975	-2.053	-1.914	-2.061	-1.883
S	.3169	.2859	.3271	.3020	.3283
δ	-115.6	—	—	-117.1	-112.8

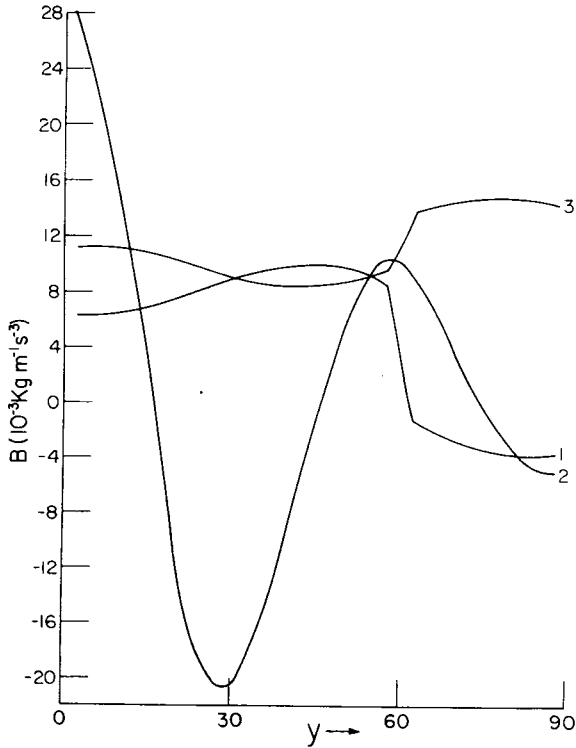


Fig. 4. Contributions of various mechanisms to the cloud cover, (1) the scaled evaporation, (2) the mean vertical velocity, (3) the diabatic heating.

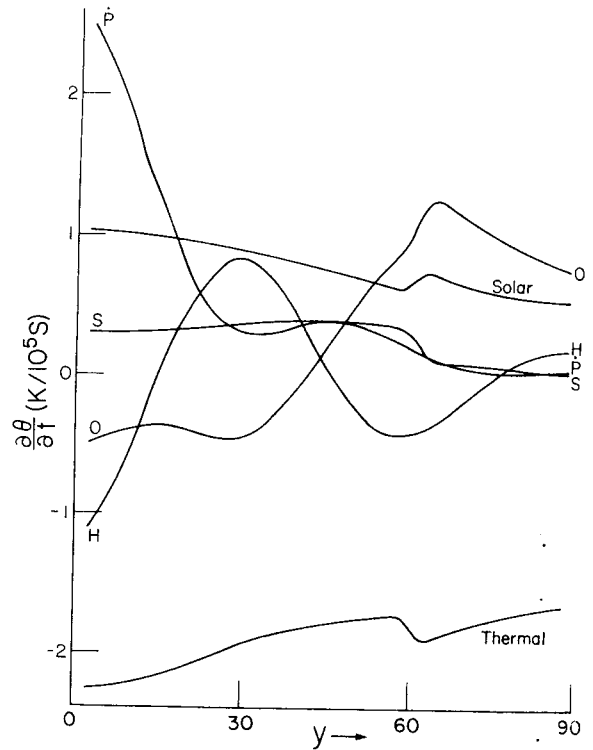


Fig. 6. The atmospheric heat balance, expressed in terms of a heating rate. Solar refers to heating by solar radiation. Thermal is infrared cooling. P and S are heating due to precipitation and surface sensible heat flux, respectively. H and O are due to the prescribed mean circulation and horizontal eddy fluxes.

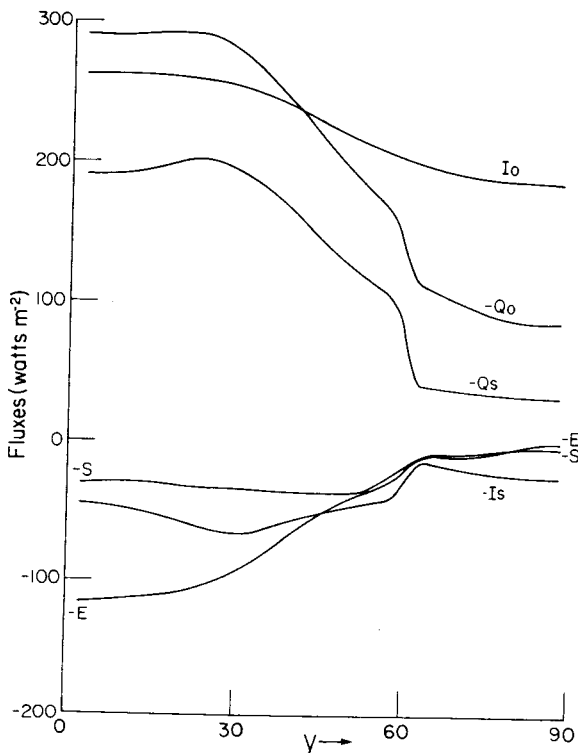


Fig. 5. The planetary radiation at the top of the atmosphere I_0 , Q_0 and the surface fluxes, I_s , Q_s , E , S .

measure the relative importance of the solar versus infrared cloud properties is (Schneider, 1972)

$$\delta = \frac{\partial(-Q_0)}{\partial C} - \frac{\partial I_0}{\partial C} \tag{17}$$

The albedo (infrared) effect dominates if $\delta < 0$ ($\delta > 0$), and an increase in cloud results in a net decrease (increase) in net downward radiation at the top of the atmosphere. Normally $(\partial(-Q_0)/\partial C) < 0$ and $(\partial I_0/\partial C) < 0$. Apart from cloud properties, δ depends also on surface albedo. Its latitudinal variation for the parameters described above is illustrated in Fig. 7; the parameter δ is negative everywhere, but much less over the ice-sheet, and so an increase in cloud cover will decrease temperatures.

Consider now the radiative equilibrium calculations. The flux balance at the top and bottom atmosphere is:

$$0 = (A\uparrow + B\uparrow T_a)(1 - C) + (A'\uparrow + B'\uparrow T_a)C + (1 - \Gamma)\sigma T^4 + Q_0 \tag{18}$$

Table 2. As in Table 1 except $\Delta S'$ refers to the experiments in which cloud cover was held constant at the control run values and $\Delta S''$ refers to the experiments in which the surface albedo was held constant at the control run values for the radioactive parameterizations only

	$\Delta S = +8$	$\Delta S = -8$	$\Delta S' = 8$	$\Delta S' = -8$	$\Delta S'' = -8$	$\Delta S'' = 8$
f	307.5	281.5	308.0	281.3	285.1	305.2
T	298.4	275.5	298.8	275.5	280.0	295.8
α_s	.1000	.2757	.1000	.2757	.1808	.1808
α_a	.2890	.3350	.2887	.3351	.3076	.3090
H	.7617	.7478	.7607	.7503	.7652	.7530
C	.5869	.5601	.5863	.5613	.5710	.5786
I_0	263.0	213.9	—	—	—	—
Q_0	-263.1	-213.8	—	—	—	—
Q_s	-176.5	-134.9	-178.0	-134.5	-145.0	-169.9
E	111.1	42.46	112.2	42.43	49.8	105.6
S	24.2	33.44	23.78	34.04	36.24	23.39
I_s	41.15	58.96	42.05	58.06	59.00	40.94
P	1.153	.4407	1.164	.4404	.5169	1.096
Solar	.889	.8197	.8969	.8211	.7857	.9231
Thermal	-2.303	-1.608	-2.308	-1.615	-1.679	-2.262
S	.2512	.3471	.2460	.3533	.3762	.2428
δ	-122.1	-106.1	—	—	—	—

$$0 = (A\downarrow + B\downarrow T_a)(1 - C) + (A'\downarrow + B'\downarrow T_a)C - \sigma T^4 + Q_s \quad (19)$$

Let us linearize T^4 about 288 K (i.e., let $T^4 \sim (288)^4 + 4(288)^3(T - 288)$). Then (18) and (19) are easily solved for T and T_a (or θ), and the results are displayed in Fig. 7. Note that the lapse rate is unstable in the tropics, but stabilizes as latitude increases, and the high surface albedo in polar regions produces a stable lapse rate. Comparison with Fig. 3 indicates that the surface fluxes and precipitation are acting to stabilize the lapse rate, and the cross latitude heat fluxes are reducing the meridional temperature gradient.

Fig. 7 also illustrates the effect of changing the cloud cover on the temperature structure, first when only changes in the infrared fluxes are allowed and then including the effects on the solar field. Note that the surface response is always greater than the atmospheric response in low latitudes. In high latitudes the high surface albedo reduces the net solar flux at the surface, and the surface and atmospheric responses are correspondingly reduced. The essential result here though is that a 1% increase in cloud cover produces a global cooling of about 0.7 K, if both solar and infrared interactions are allowed, and a much smaller cooling in high latitudes where $\delta \sim 0$.

Finally, in Fig. 8, we display the equilibrium temperatures given by the full model (i.e., when cross latitudinal and vertical heat fluxes and precipitation are included) for fixed values of cloud cover of 50% and 60% in the radiation schemes. An increase in cloud cover of 10% has caused surface temperatures to drop about 7 K and atmospheric temperatures by about 8 K. The large surface changes around 60° are due to changes in the extent of the ice sheet. Thus, we see that cloud feedback can strongly influence the global temperature, especially when this feedback is coupled to an ice-albedo feedback. However, as will be seen, the dominant cloud changes arising are local in extent and because of compensating feedbacks the cloud field has a negligible effect on the thermal climate of this model.

4. Sensitivity experiments

This section describes the effects of changing the solar constant on the climate of the model, with particular emphasis on cloud response. The change in temperature due to changes in solar constant is illustrated in Fig. 9. With ice albedo feedback, it is qualitatively similar to that found in GCM's (e.g., Wetherald and Manabe, 1975) and energy balance

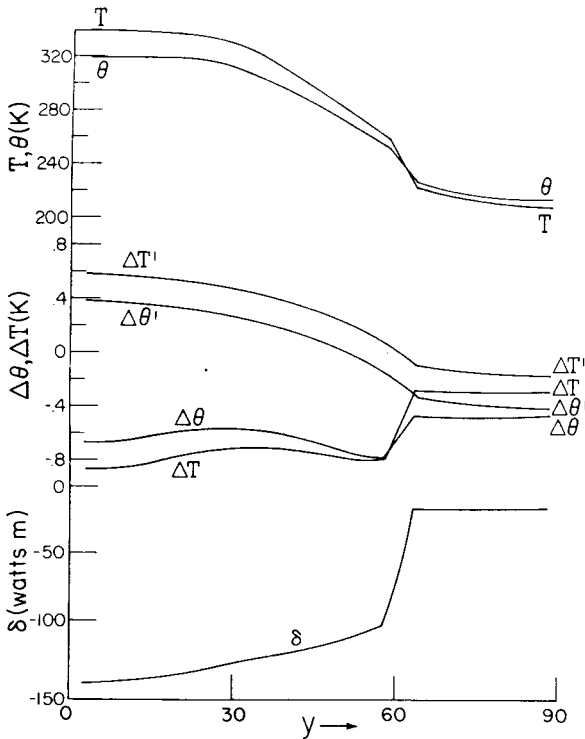


Fig. 7. Radiative parameters for the control run. T , θ refer to the radiative equilibrium values for the given surface albedo. ΔT , $\Delta\theta$ refer to the changes in this thermal structure for a 1% increase in cloud cover. $\Delta T'$, $\Delta\theta'$ refer to the changes when the cloud cover is allowed to affect only the thermal radiation. δ refers to the change in the net flux difference $-\partial F_0/\partial C$.

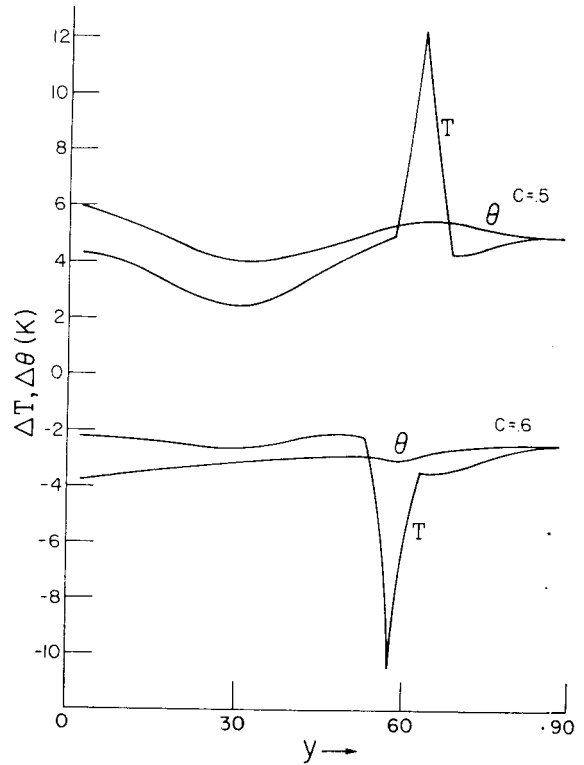


Fig. 8. The change in the temperatures (from control integration) caused by keeping cloud cover constant everywhere at $C = .5$ and $C = .6$.

models (e.g., Budyko, 1969). Quantitative differences arise between all models, mainly due to detailed differences in surface albedo specification. Clearly the cloud feedback is small and negative, whereas the ice-albedo feedback is positive and can almost double the response in high latitudes. This is the prime reason for the nonlinear change of surface temperature with solar constant. A decrease in solar constant greater than 8% is required for the earth to become ice covered, somewhat larger than many previous estimates (Budyko, 1969; Sellers, 1969; North, 1975). Numerical experiments then indicated that the earth remains ice covered until solar constant is increased to a much larger value, the hysteresis loop discussed by North (1975) and others. The surface temperature response is generally similar to, but slightly smaller than, that of the atmosphere, except in the vicinity of the edge of the ice-line where large changes occur, and the surface temperature changes are larger.

Of course, in a model such as this, quantitative simulations of the earth's climate are neither possible nor necessarily desirable, the aim being more an exploration of potentially important mechanisms. Certainly though, results should not be dependent upon small changes in parameter values. Since in this study we examine the interaction between cloud cover and the ice-line, it is necessary to show that our results are not sensitive to the precise parameters governing the position of the ice-line (cf. Saltzman and Vernekar, 1975). Fig. 10 illustrates various fields when albedo is allowed to change between 0.1 and 0.7 as temperature falls from 268 K to 258 K, pushing the ice-line polewards of its previous position. Fig. 11 shows the changes in cloud cover when solar constant is now changed by $\pm 4\%$. Results are qualitatively very similar to those obtained previously, given the change in initial ice-line position. Note, though, that an increase in solar constant of 4% is now sufficient to completely destroy the ice-sheet. For this reason the change in the cloud field is

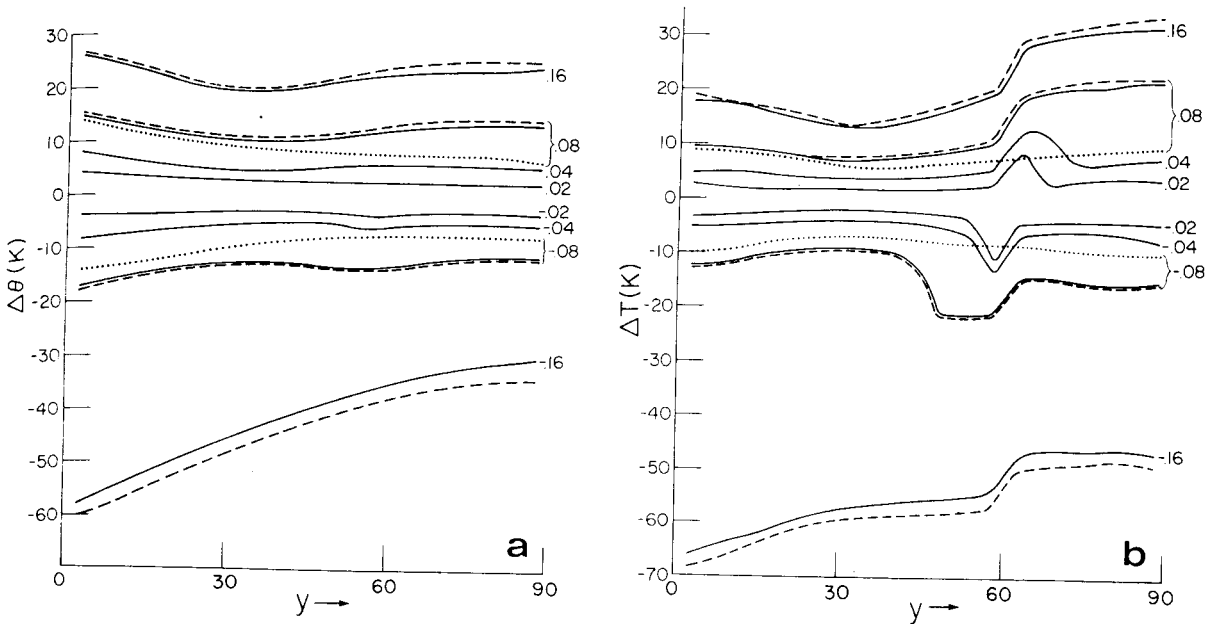


Fig. 9. (a) Changes in the atmospheric potential temperature for fractional changes in the solar constant (of ± 0.02 , 0.04 , 0.08 , 0.16). The solid lines give the results for the complete model, the dashed lines when the cloud cover for the radiative calculations was that of the control run and the dotted lines when the surface albedo was that of the control run. (b) Same as 9(a) except for the surface temperature.

monotonic polewards of the initial ice-line, as it is for an 8% increase in the original formulation.

The reason for the small feedback by the clouds can be seen from an inspection of Fig. 11. We see that in high latitudes cloud cover generally increases with solar constant, but that in low latitudes cloud cover remains essentially constant. Note especially that cloud cover increases much less in high latitudes when surface albedo is held fixed and surface temperature changes are similar to, or smaller than, the atmosphere's. As cloud cover changes predominantly in that region where its solar and infrared properties almost balance, the effect on the temperature field is small. This null effect, however, is due to our particular radiation parameterization.

It is of interest to determine the mechanisms causing the changes in this cloud cover. The simplicity of our model allows this analysis to be performed with comparative ease. As:

$$C = (\pi - \cos^{-1}(B/W))/\pi$$

then:

$$\Delta C = \frac{\Delta(B/W)}{\pi(1 - B^2/W^2)^{1/2}}$$

where:

$$\left\{ \Delta \left(\frac{B}{W} \right) \right\} = \{ \Delta B_1 + \Delta B_2 + \Delta B_3 + \Delta B_4 + \Delta B_5 + \Delta B_6 \} / W$$

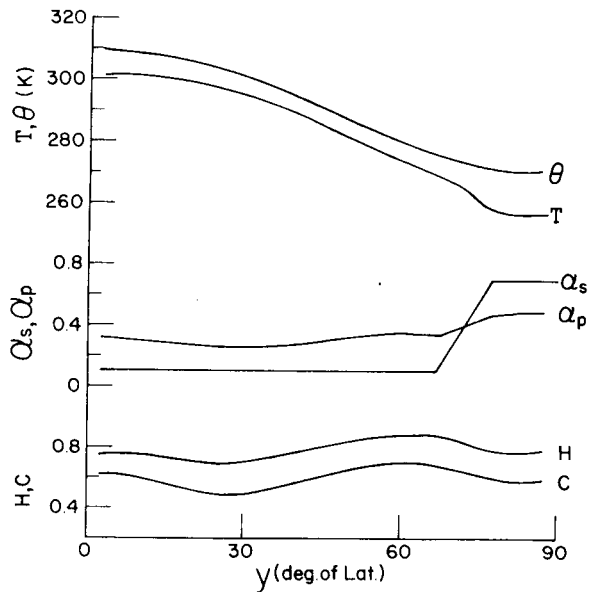


Fig. 10. As for Fig. 3, but for run with ice forming only at 268 K (instead of 273 K). Vertical velocity is same as in Fig. 3.

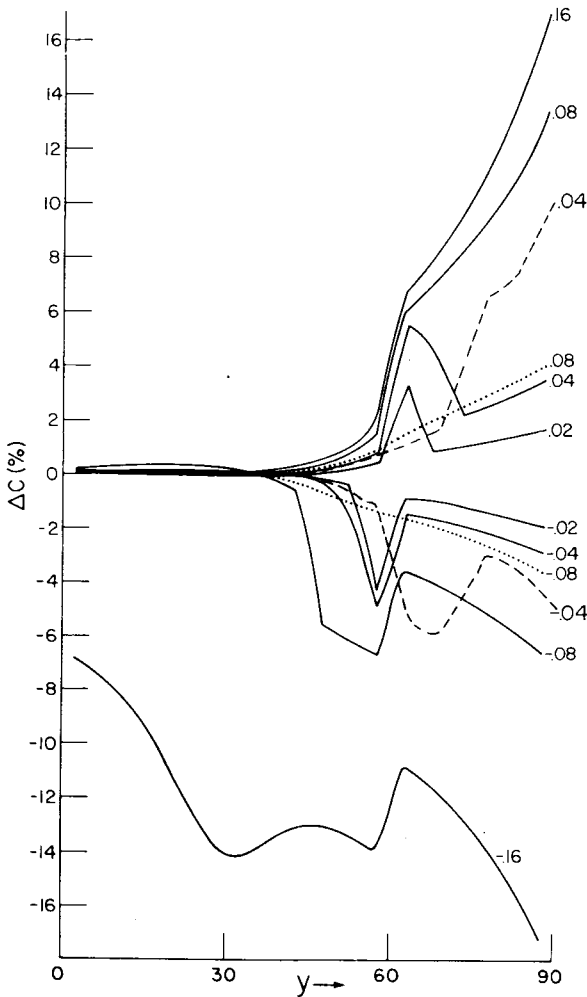


Fig. 11. Changes in the cloud cover for fractional changes in solar constant. The dotted lines refer to fixed surface albedo. The dashed lines refer to the experiment with ice forming at 268 K. Solid lines use control model. Change in solar constant is marked on each curve.

and:

$$\Delta B_1 = \frac{3C_D(\Delta q_v)}{q_\beta}$$

$$\Delta B_2 = -\frac{3C_D q_v \Delta q_\beta}{q_\beta^2}$$

$$\Delta B_3 = -\frac{\Delta q_\alpha}{q_\beta} \frac{g}{C_p} \xi(F_s - F_0 - S)$$

$$\Delta B_4 = \frac{q_\alpha \Delta q_\beta}{q_\beta^2 C_p} \xi \Delta(F_s - F_0 = S)$$

$$\Delta B_5 = -\frac{q_\alpha g}{q_\beta C_p} \xi \Delta(F_2 - F_0 - S)$$

$$\Delta B_6 = -\frac{B \Delta W}{W^2}$$

Fig. 12 shows the various contributing factors. ΔB_1 is the lapse rate effect, ΔB_5 is the effect of the change in the diabatic heating, and ΔB_6 is the effect of any change in vertical velocity (zero in this model). ΔB_2 , ΔB_3 and ΔB_4 are changes in the relative humidity thermodynamic coefficients. In low latitudes ΔB_1 is negative with increasing temperature, due to a stabilization of the lapse rate. This is largely compensated for by an increase in B_5 ; increased precipitation and temperatures causes more infrared cooling. Other terms are generally small. In high latitudes the lower atmosphere is destabilized because of the surface albedo change, and this is the dominant cause of increased cloud cover (note the much smaller change in B_5 when albedo is fixed (Fig. 12c). The coefficients ΔB_2 , ΔB_3 and ΔB_4 are always small and cloud cover changes are due primarily to changes in the lower-level static stability and atmospheric heating.

Thus, even though cloudiness has the potential for strongly feeding back on the model, the effects are small. This is due to negligible changes in cloud cover in low latitudes (where radiative feedback is stronger) and small radiative feedbacks in high latitudes where cloud changes are large.

5. Concluding comments

We have attempted to analyze in some detail a relatively simple two-level energy balance climate model with a cloud parameterization, partly to aid understanding of the cloud responses in various GCM integrations.

It was found that with an increase in solar constant the ice sheet retreated, the lower atmosphere (in high latitudes) was destabilized and an increase in scaled surface evaporation caused increased cloud cover. However, because of compensating feedbacks by thermal and solar radiation, the net radiative feedback was very small.

In lower latitudes an increased solar constant stabilized the lower atmospheric lapse rate due to increased evaporation which required a smaller vertical flux of sensible heat. The direct analog of this mechanism in the atmosphere away from the surface is the decrease in wet adiabatic lapse rate with increasing temperature. In spite of the absolute evaporation increasing, the scaled evaporation

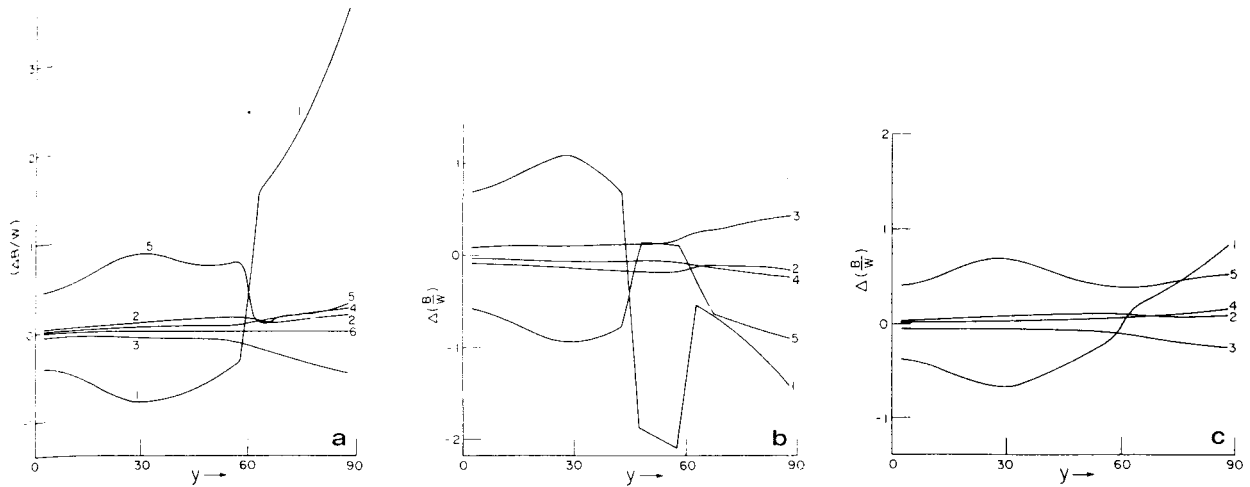


Fig. 12. (a) The changes in the various terms ($\Delta B_1 \dots \Delta B_6$) that contribute to the cloud cover changes in the experiment with an 8% increase in solar constant. (b) As in 12(a) except for 8% decrease solar constant. (c) As in 12(a) except here α_s was the same as in the control run.

(which describes the influence of evaporation on the cloud field) actually decreased. Acting alone this would cause the cloud field to drop. However, this was largely compensated for by an increase in the net radiative cooling (required to balance the increased precipitation) which acts to increase cloud cover.

Thus, the impact of cloud feedback in the model is small. However, in order to make a tractable energy balance model and to provide insight, various simplifications have been made. This study has focused on the influence of changes in surface fluxes and surface albedo and eliminated the feedbacks from changes in eddy vertical velocity and mean circulation. Yet the changes in low-level cloud cover and temperature with a change in solar constant do resemble the results found in the comprehensive GCM of Wetherald and Manabe (1980). Furthermore, the parameterizations within the model are based on physical theories and yield an equilibrium climate, temperature, precipitation, cloud cover, similar to the observed. These arguments do strongly suggest that such changes in the GCM, and, by extension, the real atmosphere, are due to mechanisms connected to the lapse rate as described above.

It should be noted that the model does not allow eddy and zonal mean vertical velocity fields to be determined internally. In some model studies (e.g., Roads, 1978a) an increase in temperature increases the intensity of the hydrologic cycle, increases the eddy vertical velocity variance and the fractional

cloud cover is reduced. If this mechanism were to exist in our model, cloud cover would feed back positively on any change in temperature. We have also only attempted to predict one level of cloud cover, and are, thereby, unable to predict any effects involving a change in cloud-top height, potentially of major importance. Finally, changes in the cloud optical properties may also have a large influence (e.g. Temkin et al., 1975).

Perhaps the next stage for understanding the large-scale cloud cover and its influence on the radiation field is via the use of a model with an internally consistent calculation of the vertical velocities. Such a model would need some degree of longitudinal structure and more vertical structure while ideally retaining the essential simplicity of this model. An attempt along these lines is reported on in Roads et al. (1983).

6. Acknowledgements

This research was sponsored in part by California Space Institute (CalSpace grant #CS08-81). Support for J. Roads was also provided by National Aeronautics & Space Administration (NASA grant NAG5-105). We also gratefully acknowledge the computer programming of Lorraine Remer, the text-editing of Grace Johnston, and the figure drafting of Fred Crowe and his group. Helpful comments on the manuscript were also given by D. Cayan. We thank an anonymous referee for constructive comments.

REFERENCES

- Budyko, M. I. 1969. The effect of solar radiation variations in the climate of the earth. *Tellus* 21, 611–619.
- Cess, R. D. 1976. Climate change: An appraisal of atmospheric feedback mechanisms employing zonal climatology. *J. Atmos. Sci.* 33, 1831–1843.
- Cess, R. D. and Ramanathan, V. 1978. Averaging of infrared cloud opacities for climate modeling. *J. Atmos. Sci.* 35, 919–922.
- Cess, R. D., Briegleb, B. P. and Liam, M. S. 1982. Low latitude cloudiness climate feedback. Comparative estimates from satellite data. *J. Atmos. Sci.* 39, 53–59.
- Green, J. S. A. 1970. Transfer properties of the large scale eddies and the general circulation of the atmosphere. *Q. J. R. Meteorol. Soc.* 96, 157–185.
- London, J. 1957. A study of the atmospheric heat balance. Final Report, AFCRC contract AF19(122)-16S, New York University, 99 pp [BBC AD 117227].
- MacCracken, M. C. 1969. Ice age theory analysis by computer model simulation. Ph.D. thesis, University of California, Davis, 193 pp.
- Manabe, S. and Wetherald, R. T. 1975. The effects of doubling the CO₂ concentration on the climate of a general circulation model. *J. Atmos. Sci.* 32, 3–15.
- Meleshko, V. P. and Wetherald, R. T. 1981. The effect of a geographical cloud distribution on climate: A numerical experiment with an atmospheric general circulation model. *J. Geophys. Res.* 8, 11995–12019.
- Namias, J. 1960. Factors in the initiation, perpetuation and termination of drought. Extract of Publication No. 51 of the I.A.S.H. commission of Surface Waters, 81–94.
- North, G. R. 1975. Analytical solution to a simple climate model with diffusive heat transport. *J. Atmos. Sci.* 31, 1301–1307.
- Ohring, G. and Clapp, P. 1980. The effect of changes in the cloud amount on the net radiation at the top of the atmosphere. *J. Atmos. Sci.* 37, 447–454.
- Paltridge, G. W. 1975. Global dynamics and climate change—a system of minimum entropy exchange. *Q. J. R. Meteorol. Soc.* 101, 475–484.
- Paltridge, G. W. and Platt, C. M. R. 1976. *Radiative Processes in Meteorology and Climatology*, Elsevier Scientific Publishing Co.
- Potter, G. L., Ellsaesser, H. W., MacCracken, M. C. and Mitchell, C. S. 1981. Climate change and cloud feedback: The possible radiative effects of latitudinal redistribution. *J. Atmos. Sci.* 38, 489–493.
- Roads, J. O. 1978a. Numerical experiments on the climatic sensitivity of an atmospheric hydrologic cycle. *J. Atmos. Sci.* 35, 753–773.
- Roads, J. O. 1978b. Relationships among fractional cloud coverage, relative humidity and condensation in a simple wave model. *J. Atmos. Sci.* 35, 1450–1462.
- Roads, J. O., Vallis, G. K. and Remer, L. 1983. Cloud/climate sensitivity experiments. Proc. 4th Biennial Ewing Symposium, in press.
- Rodgers, C. D. 1967. The radiative heat budget of the troposphere and lower stratosphere. Planetary Circulation Project, Report No. A2, M.I.T., 104 pp, [NTIS PB-176 527].
- Saltzman, B. and Vernekar, A. D. 1978. A solution for the Northern Hemisphere climatic zonation during a glacial maximum. *Quaternary Res.* 5, 307–320.
- Schneider, S. H. 1972. Cloudiness as a global climate feedback mechanism. The effects on the radiation balance and surface temperature of variations in cloudiness. *J. Atmos. Sci.* 29, 1413–1422.
- Schneider, S. H., Washington, W. M. and Chervin, R. M. 1978. Cloudiness as a climate feedback mechanism: Effects on cloud amounts of prescribed global and regional surface temperature changes in the NCAR GCM. *J. Atmos. Sci.* 35, 2207–2221.
- Sellers, W. B. 1969. A global climatic model based on the energy balance of the earth-atmosphere system. *J. Appl. Meteorol.* 8, 392–400.
- Sellers, W. B. 1976. A two-dimensional global climate model. *Mon. Wea. Rev.* 104, 233–248.
- Smagorinsky, J. 1963. General circulation experiments with the primitive equations: I. The basic experiment. *Mon. Wea. Rev.* 91, 99–164.
- Temkin, R. L., Weare, B. C. and Snell, F. M. 1975. Feedback coupling of absorbed solar radiation by three model atmospheres with clouds. *J. Atmos. Sci.* 32, 873–880.
- Vallis, G. K. 1982. A statistical-dynamical climate model with a simple hydrology cycle. *Tellus* 34, 211–227.
- Vernekar, A. D. 1979. Variations in insolation caused by changes in orbital elements of the earth. In: *The solar output and its variations*, O. R. White (ed), CAUP, Boulder, CO.
- Weare, B. C. and Snell, F. M. 1974. A diffuse thin atmosphere structure as a feedback mechanism in global climate modeling. *J. Atmos. Sci.* 31, 1725–1734.
- Wetherald, R. T. and Manabe, S. 1975. The effect of changing the solar constant on the climate of a general circulation model. *J. Atmos. Sci.* 32, 2044–2059.
- Wetherald, R. T. and Manabe, S. 1980. Cloud cover and climate sensitivity. *J. Atmos. Sci.* 37, 1485–1510.